

Article

Synthesis and Physicochemical Properties of [(1R,2S,5R)-2-isopropyl-5-methylcyclohexyloxy]-thiophen-5-yl-substituted Tetrapyrizinoporphyrazine with Magnesium(II) Ion

 Sebastian Lijewski ¹, Jiří Tydlitát ^{2,*} , Beata Czarczynska-Goslinska ³, Milan Klikar ² , Jadwiga Mielcarek ⁴, Tomasz Goslinski ¹  and Lukasz Sobotta ^{4,*} 

- ¹ Department of Chemical Technology of Drugs, Poznan University of Medical Sciences, Grunwaldzka 6, 60-780 Poznan, Poland; slijewski@ump.edu.pl (S.L.); tomasz.goslinski@ump.edu.pl (T.G.)
- ² Institute of Organic Chemistry and Technology, Faculty of Chemical Technology, University of Pardubice, Studentská 573, CZ-532 10 Pardubice, Czech Republic; milan.klikar@upce.cz
- ³ Department of Pharmaceutical Technology, Poznan University of Medical Sciences, Grunwaldzka 6, 60-780 Poznan, Poland; bgoslinska@ump.edu.pl
- ⁴ Department of Inorganic and Analytical Chemistry, Poznan University of Medical Sciences, Grunwaldzka 6, 60-780 Poznan, Poland; jmielcar@ump.edu.pl
- * Correspondence: Jiri.Tydlitat@upce.cz (J.T.); lsobotta@ump.edu.pl (L.S.)



Citation: Lijewski, S.; Tydlitát, J.; Czarczynska-Goslinska, B.; Klikar, M.; Mielcarek, J.; Goslinski, T.; Sobotta, L. Synthesis and Physicochemical Properties of [(1R,2S,5R)-2-isopropyl-5-methylcyclohexyloxy]-thiophen-5-yl-substituted Tetrapyrizinoporphyrazine with Magnesium(II) Ion. *Appl. Sci.* **2021**, *11*, 2576. <https://doi.org/10.3390/app11062576>

Academic Editors: Susana Santos Braga and Emmanuel A. Theodorakis

Received: 6 February 2021
Accepted: 9 March 2021
Published: 13 March 2021

Publisher's Note: MDPI stays neutral with regard to jurisdictional claims in published maps and institutional affiliations.



Copyright: © 2021 by the authors. Licensee MDPI, Basel, Switzerland. This article is an open access article distributed under the terms and conditions of the Creative Commons Attribution (CC BY) license (<https://creativecommons.org/licenses/by/4.0/>).

Abstract: Tetrapyrizinoporphyrazine with peripheral menthol-thiophenyl substituents was synthesized using Linstead conditions and purified by flash column chromatography. The optimized synthetic and purification procedures allowed us to obtain a new macrocycle with 36% yield. Tetrapyrizinoporphyrazine derivative was characterized by UV–Vis and NMR spectroscopy, as well as MS spectrometry. Complex NMR studies using 1D and 2D NMR techniques allowed the analysis of the bulky menthol-thiophenyl substituted periphery of the new macrocycle. Further, photochemical stability and singlet oxygen quantum yield were determined by indirect method with diphenylisobenzofuran. The new tetrapyrizinoporphyrazine revealed low generation of singlet oxygen with a quantum yield of singlet oxygen formation at 2.3% in dimethylformamide. In turn, the macrocycle under irradiation with visible light presented very high stability with quantum yield for photostability of 9.59×10^{-6} in dimethylformamide, which figures significantly exceed the border for its classification as a stable porphyrinoid (10^{-4} – 10^{-5}).

Keywords: menthol; photostability; phthalocyanines; singlet oxygen; terpenes

1. Introduction

Phthalocyanines (Pcs) are synthetic, tetrapyrrolic macrocycles revealing interesting physicochemical properties and many practical applications in technology [1]. Pcs have been successfully utilized as green chemistry catalysts for electrochemical reduction of CO₂ [2,3] or as components in alkaline membrane fuel cells [4]. Moreover, Pcs are considered useful materials for chemical sensors, non-linear optics applications, and data storage [5]. One of the unique features of Pcs is their ability to generate singlet oxygen and other reactive oxygen species upon excitation with visible light. Therefore, Pcs have been applied or at least considered as promising candidates for photosensitizers (PSs) in photodynamic therapy (PDT) and photodynamic antimicrobial chemotherapy (PACT) [6–8]. Tetrapyrizinoporphyrazines constitute a distinct class of Pcs aza-analogues. Both metal-free tetrapyrizinoporphyrazines and their metal complexes have demonstrated interesting optical and electrochemical properties and also potential applications in technology and medicine [9–16]. Tetrapyrizinoporphyrazines similarly to Pcs reveal comparable abilities to generate singlet oxygen [17]. Moreover, they exhibit excellent electrochemical properties, which make their application in Li/SOCl₂ batteries possible and has resulted in improved performance in terms of their capacity and discharge voltage [18].

Implementing a thiophene moiety into the designed macrocycle was related to encouraging reports on photosensitizers substituted with this heterocycle in the periphery. Brominated BODIPYs with thiophene rings were studied as potential photosensitizers for photodynamic therapy using a low irradiance excitation [19]. The presence of thiophene rings significantly influenced the red-shifts in their absorption maxima. In another study, halogenated thieno[3,2-*b*] thiophene fused BODIPY revealed not only long wavelength absorptions at maximum up to 720 nm but also photocytotoxicity upon irradiation with light NIR laser in living HeLa cells [20]. In the study performed by Bai et al., a near-infrared and lysosomal targeting thiophene-BODIPY photosensitizer was studied in terms of its photocytotoxicity against A549 cancer cells [21]. Moreover, Önal et al. revealed photoinduced anti-inflammatory activities of a thiophene-substituted subphthalocyanine derivative on mammalian macrophages *in vitro* [22]. They noted this compound's influence on the extracellular levels of inflammatory cytokines and their gene expression levels. Studies that have been presented so far for various phthalocyanines and porphyrazines revealed the potential of thiophene rings in the modification of their physicochemical properties. Chen et al. reported that conjugating thiophene ring with phthalocyanine systems could significantly improve their multi-proton absorption cross-section [23], which can be of value for potential applications of these macrocycles in the third-order nonlinear optics. In another study, a self-assembled monolayer of cobalt thiopheneethoxy-substituted phthalocyanine presented interesting electrocatalytic behavior towards catalytic oxidation of thiocyanate, L-cysteine, and 2-mercaptoethanol [24]. Many papers have been published on porphyrazines with annulated strongly electron-withdrawing thia- and selenodiazole rings, which revealed distinct structural, electronic, UV-Vis spectroscopic, and electrochemical features [25]. Unfortunately, there are few examples of porphyrazines containing 5-membered heteroaromatic rings substituted directly to the β -position of the macrocyclic system. One example is a coplanar binuclear magnesium(II) porphyrazine bearing six bis-(trimethylthiophenyl) photochromic functionalities at the periphery, which was considered as a molecule of potential applications for technology in information data storage, and as a component of imaging devices and switches [26]. Other examples, obtained in our group, are unsymmetrical porphyrazines containing mixed dithienylpyrrolyl and dimethylamino groups in the periphery, which were subjected to structural and spectroscopic characterization [27]. Among azaphthalocyanine macrocycles, worth noting are zinc(II) azaphthalocyanines with thiophen-2-yl, 5-methylthiophen-2-yl, and pyridine-3-yl peripheral substituents, which were obtained and subjected to physicochemical study by Mørkved and Zimcik [28].

Conjugation of biologically active compounds from different chemical groups is one of the modern drug development approaches. Various molecular consortia appeared to be useful in the drug development process and brought the desired biological effect [29]. In the literature, many other molecular consortia consisting of menthol and photosensitizers can be found, which compounds revealed interesting technological and biological properties. For example, menthol was tagged with BODIPY (borondipyrromethane) in search of fluorescence biological markers [30,31]. Lately, Lv et al. presented "pinwheel-like" phthalocyanines with four (D)- or (L)-menthol units at non-peripheral positions and assessed their spectroscopic and electrochemical properties [32]. Romero et al. studied photophysical and photodynamic activity of zinc(II) phthalocyanine-menthol ((1S,2R,5S)-2-isopropyl-5-methylcyclohexyloxy) conjugate, which was incorporated in micelles of 12 different surfactants. The lipophilic conjugate incorporated in Pluronic[®] F-127 formulation was found to be an ideal drug delivery system for this PS [33]. It is worth noting that introducing a bulky menthol substituent to the phthalocyanine periphery was also found as an aggregation reducing factor [34]. The rationale for our approach resulted from our former study in which there were obtained biologically active terpene-macrocyclic conjugates, composed of thymol or carvacrol and phthalocyanine. In that study, these conjugates were synthesized, characterized, loaded into modified liposomes, and subjected to detailed optical and biological experiments. Thymol-phthalocyanine conjugate at both 100 and

10 μm concentrations revealed high, ca. 5 log photoinactivation potential on the growth of *Enterococcus faecalis* [35].

Interest in menthol as a component of molecular consortia is related to its unique medical properties. Menthol, 5-methyl-2-(1-methylethyl)cyclohexanol, is a cyclic monoterpene with three asymmetric carbon atoms. It occurs as four pairs of optical isomers. What is more, it can be isolated from the mint leaves essential oil and has been used in traditional medicine since ancient times. Menthol is utilized in pharmaceuticals, confectionery, hygiene products, cosmetics, and pesticides [36,37]. Moreover, it has been widely used as a food additive and in cosmetics due to its taste and cooling sensation. Its cooling properties enables the application of menthol as a topical analgesic [38]. In medicine, menthol is known for its antioxidant, anti-inflammatory, and analgesic activity [37]. Like many terpenes, menthol exhibits intense antimicrobial activity against various microorganisms, including bacteria and fungi [39]. Moreover, there are many examples of synergistic responses when combinations of monoterpenes with antibiotics are studied. Kifer et al. researched the antimicrobial potency of single and combined mupirocin with various monoterpenes. They found that the application of the monoterpene–menthol with antibiotic-mupirocin could potentiate the antimicrobial activity according to the synergism pathway. In addition, they suggested that menthol loosens the bacterial membrane making it prone to be crossed by various molecules, including photosensitizers [40].

The use of both menthol and thiophene fragments attached to the porphyrinoid core can be considered as a significant factor modifying the physicochemical properties of the desired terpene-macrocycle conjugates and influence their potential applications in technology and medicine. Therefore, in our current study, we decided to apply the methodology related to molecular consortia synthesis to other structurally relevant macrocycles, which are tetrapyrazinoporphyrazines and equip these molecules with bulky substituents containing thiophen-5-yl part and menthol.

2. Materials and Methods

2.1. General Procedures

All reactions were carried out in oven-dried glassware under an argon atmosphere using the Radleys Heat-On heating system. All solvents were evaporated at or below 50 °C under reduced pressure. Flash column chromatography was carried out on Merck silica gel, particle size 40–63 μm . Reversed-phase chromatography was carried out on Fluka C18 silica gel 90 (particle size 40–63 μm). Thin-layer chromatography (TLC) was made on silica gel Merck Kieselgel 60 F254 plates and visualized with UV illumination (λ max 254 or 365 nm). UV–Vis spectra were measured on a Hitachi UV/VIS U-1900 spectrophotometer. ^1H NMR, ^{13}C NMR spectra were recorded using a Bruker Avance III spectrometer working at 500.25 MHz for ^1H and 125.79 MHz for ^{13}C at the Institute of Bioorganic Chemistry Polish Academy of Sciences in Poznan. Chemical shifts (δ) are quoted in parts per million (ppm) and referred to a residual solvent peak, whereas coupling constants (J) are quoted in Hertz (Hz). The abbreviations s, d, m refer to a singlet, doublet, and multiplet, respectively. Mass spectra were measured at Bruker MALDI TOF/TOF UltrafleXtreme mass spectrometer at the Wielkopolska Centre for Advanced Technologies in Poznan.

2.2. Synthetic Procedures

5,6-Bis(2-[(1R,2S,5R)-2-isopropyl-5-methylcyclohexyloxy]-thiophen-5-yl)pyrazine-2,3-dicarbonitrile **1** was synthesized according to a literature method [41].

Magnesium(II) 2,3,9,10,16,17,23,24-octakis{2-[(1R,2S,5R)-2-isopropyl-5-methylcyclohexyloxy]-thiophen-5-yl}-1,4,8,11,15,18,22,25-(octaaza)phthalocyanine

Magnesium turnings (2 mg, 0.083 mmol), a small crystal of iodine and *n*-butanol (1 mL) were refluxed for 4 h. After the mixture was cooled to room temperature, compound **1** (50 mg, 0.083 mmol) was added. The reaction mixture was refluxed for 20 h. The solvent

was evaporated with toluene and the residue was dissolved in dichloromethane and chromatographed (CH₂Cl₂: MeOH; 50:1 to 10:1 *v/v*) to give a dark blue film of azaphthalocyanine **2** (18 mg, 36%):

Rf (CH₂Cl₂: MeOH, 10:1 *v/v*) 0.26; UV-Vis λ (log ϵ); 405 nm (3.71), 663 nm (4.33). MS (MALDI) *m/z* calcd. for C₁₃₆H₁₆₈MgN₁₆O₈S₈:2434.0919 [M+H]⁺; found: 2434.0924. ¹H NMR (500.25 MHz, pyridine-*d*₅) δ 7.96 (s, 8H, Th), 6.69 (s, 8H, Th), 4.33 (s, 8H, Menth), 2.57 (s, 8H, Menth), 2.49 (s, 8H, Menth), 1.79 (s, 8H, Menth), 1.77 (s, 8H, Menth), 1.72 (s, 8H, Menth), 1.60 (s, 16H, Menth), 1.29 (s, 8H, Menth), 1.23 (s, 8H, Menth), 1.12 (s, 24H, Menth), 1.07 (s, 24H, Menth), 1.06 (s, 24H, Menth), 0.99 (s, 8H, Menth). ¹³C NMR (125.8 MHz, pyridine-*d*₅) δ 170.0, 151.8, 148.6, 148.1, 130.4, 129.1, 108.4, 86.0, 48.8, 41.0, 35.0, 32.1, 27.2, 24.4, 22.8, 21.5, 17.5.

2.3. Measurement of Singlet Oxygen Quantum Yield

Singlet oxygen quantum yield was measured in dimethylformamide (DMF) solution under aerobic conditions. It was performed according to a previously described method [42–46]. 1,3-Diphenylisobenzofuran (DPBF) was applied as a singlet oxygen chemical quencher. The unsubstituted zinc(II) phthalocyanine (ZnPc) was used as a reference. The mixture of DPBF and photosensitizer was irradiated with monochromatic light at the wavelength adjusted to the maximum of Q band in the absorption spectrum. The UV-Vis spectrum was recorded during the measurements in equal time intervals. Finally, DPBF decomposition kinetics was calculated and compared with the reference.

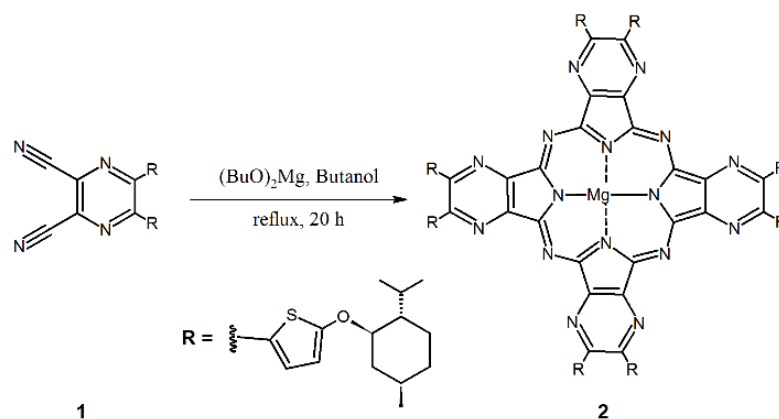
2.4. Determination of Photostability Quantum Yield

Photostability evaluation was performed by irradiation of solution containing studied compound with light at the wavelengths above 450 nm in DMF. During irradiation at specified time intervals, the UV-Vis spectra were measured. The calculations of quantum yields were performed according to the method presented earlier [44,47–49].

3. Results and Discussion

3.1. Synthesis and Characterization

The menthoxy-thiophenyl functionalized dicyanopyrazine **1** was synthesized and characterized following lately published procedure [41]. The conjugate **1** was subjected to the Lindsey macrocyclization reaction using magnesium *n*-butanolate as a base in *n*-butanol (Scheme 1). After refluxing the reaction mixture for 20 h, thin layer chromatography was made and revealed the formation of a distinct dark blue colour macrocycle. Multiple flash column chromatography was performed on a silica gel as the stationary phase using a mixture of dichloromethane and methanol as the mobile phase. New tetrapyrroloporphyrin with peripheral menthol-thiophenyl substituents **2** was purified and isolated with 36% yield.



Scheme 1. Synthesis of azaphthalocyanine **2** conjugate.

Conjugate **2** was characterized using mass spectrometry, NMR spectroscopy (including one- and two-dimensional techniques) and UV–Vis spectrophotometry. In the MALDI mass spectrum of the novel conjugate, a quasimolecular ion m/z 2434 formed by the addition of a proton was found.

Various NMR 1D and 2D techniques, accompanied by literature data allowed to assign hydrogens and carbons to signals appearing in the ^1H and ^{13}C NMR spectra. There were not many correlations present in the ^1H – ^1H COSY and ^1H – ^{13}C HMBC NMR spectra. Therefore, signals resulting from the hydrogens belonging to cyclohexane ring (b–f, Figure 1) were assigned following the data obtained in the study and analyzed together with that previously obtained by other authors. It concerns especially Lv et al. who performed a study for structurally similar phthalocyanine with four (D)- or (L)-menthol units at non-peripheral positions [32], as well as conformational analysis made by Härtner et al. for menthol diastereomers using NMR and DFT computation [50]. The effects observed in the NMR spectra related to coupling constants and correlation spots were the result of dihedral torsion angles between vicinal hydrogens within cyclohexane-menthoxy chair conformation and reflected the Karplus equation [51]. In the ^1H NMR spectrum of **2** two distinct singlets were found in the aromatic region at 7.96 and 6.69 ppm, which originate from thiophene ring protons (t). In the ^1H NMR spectrum signal of the aliphatic hydrogen atom (a) at carbon atom participating in the ether bond was observed at 4.33 ppm. At ca. 2.5 ppm, two close singlets were noted. The signal at 2.57 ppm belongs to f hydrogens in the cyclohexane ring, located between ether bond carbon and tertiary carbon linked to the methyl group. The signal at 2.49 ppm was assigned to the j hydrogens linked with tertiary carbon within the isopropyl group. Both signals mentioned above exhibit similar integration, which confirms that hydrogens at f position appear in axial and equatorial positions and that the signal at 2.57 ppm results from one of two protons only. Another close signals pair appears in the ^1H NMR at 1.79, and 1.77 ppm and belongs to adjacent c and d hydrogens in the cyclohexane ring. The above-mentioned signals result from one of two hydrogens only, which are present in these positions. The signals from b and e hydrogens at the tertiary carbon atoms of the substituted cyclohexane ring appeared at 1.72 and 1.60 ppm, respectively. Poorly distinguished multiplets at 1.29 ppm, 1.23 ppm, and 0.99 ppm represent the second of the f, c and d hydrogens, respectively. According to the signal integration, the peak appearing at 1.12 ppm was assigned to h methyl group protons within the isopropyl group, and it represents only one of two methyl groups present within this moiety. Close singlets appearing at 1.07 and 1.06 ppm represent two distinguished methyl groups of which the signal at 1.07 ppm represents the second of the h methyl groups within the isopropyl moiety, whereas the signal at 1.06 ppm corresponds to the methyl group g hydrogens. The NMR spectra were also included in the Supporting Information.

According to the expectations, in the ^1H NMR spectrum, the protons in the cyclohexane ring of menthoxy moiety appearing at equatorial and axial positions were present at various chemical shifts confirming the presence of two populations of signals originating from two different population of hydrogens. Such a phenomenon was also noted in the ^1H – ^{13}C HSQC NMR spectrum (Figure 2), where the hydrogen signals at 1.77, 1.23 ppm (c position of the cyclohexane ring) were correlated with the same carbon atom at 24.4 ppm. Similarly, pairs of hydrogens appearing at 1.77, 0.99 ppm (d position of cyclohexane ring) and at 2.57, 1.29 ppm (f position) were correlated with carbon atoms at 35.0 ppm and 41.0 ppm, respectively. In the ^1H – ^{13}C HSQC NMR spectrum very close proton signals at 1.07 ppm and 1.06 ppm present at two different cyclohexane ring substituents were also distinguished, which is also in agreement with the data lately reported by Zeng et al. [52].

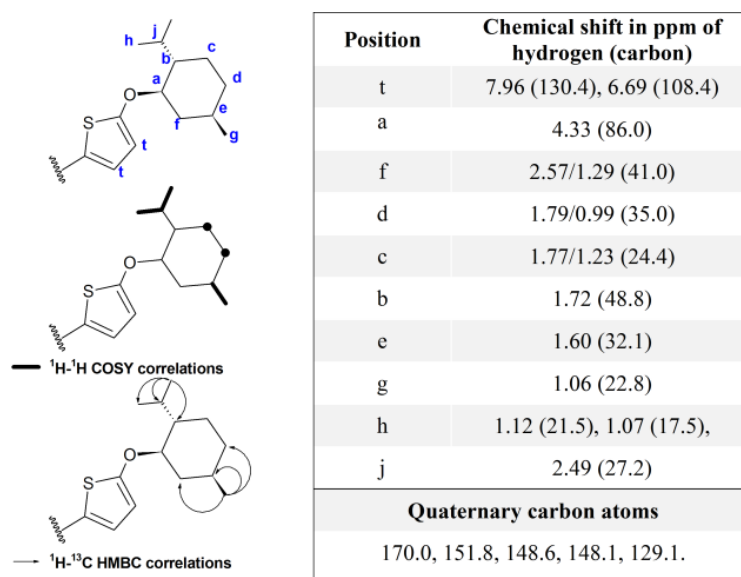


Figure 1. Signals for hydrogen and carbon atoms of **2** according to NMR spectroscopy and correlations observed in two-dimensional COSY, HSQC, and HMBC experiments; COSY—Correlation Spectroscopy, HSQC—Heteronuclear Single Quantum Correlation, HMBC—Heteronuclear Multiple Bond Correlation.

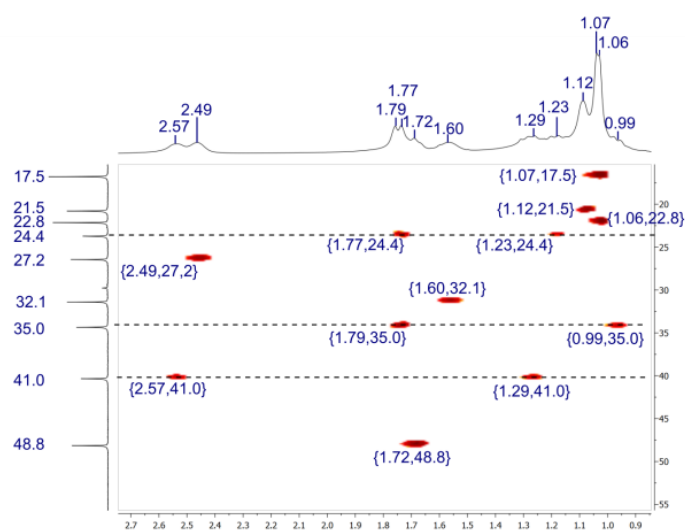


Figure 2. Fragment of ^1H - ^{13}C HSQC NMR spectrum of **2** in pyridine- d_5 .

The ^1H - ^1H COSY NMR spectrum of **2** revealed correlations between hydrogens within the isopropyl group and c and d vicinal hydrogens. Further, the correlation of signals at 1.60, 1.06 ppm proved proximity of e and g hydrogens (Figure 3).

In the ^1H - ^{13}C HMBC NMR spectrum of the obtained conjugate, a few long-range heteronuclear correlations were observed (Figure 4), which allowed us to assign hydrogen signals at 1.07 and 1.06 ppm to the methyl group within the isopropyl substituent and 5-methyl group, respectively.

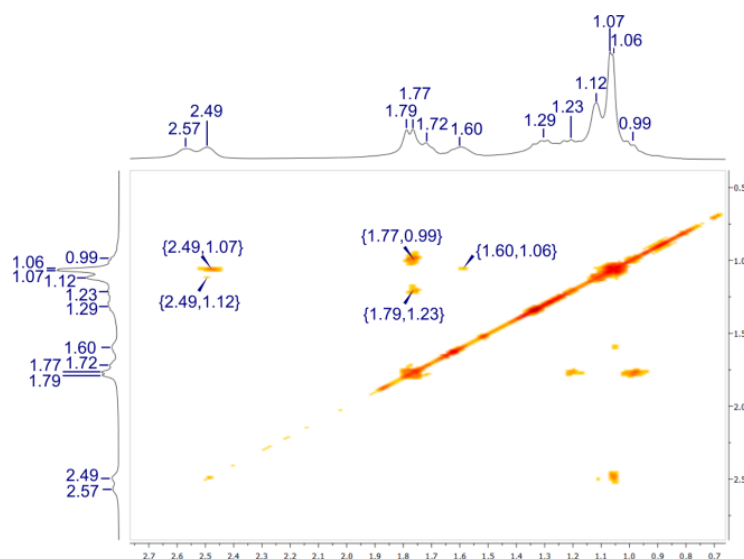


Figure 3. Fragment of ^1H - ^1H COSY NMR spectrum of **2** in pyridine- d_5 .

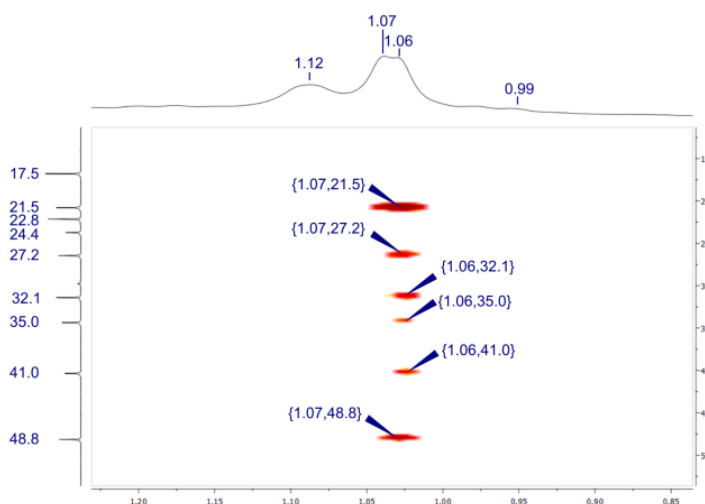


Figure 4. Fragment of ^1H - ^{13}C HMBC NMR spectrum of **2** in pyridine- d_5 .

3.2. Photochemical Properties

In the UV-Vis spectrum of **2** two absorption bands were noted. The spectrum profile is typical for azaphthalocyanines, with the Soret band in the range of 300–460 nm and the Q band located in the range of 600–750 nm (Figure 5). These bands arise from the π - π^* transitions. Slightly increased absorption in the range of 500–600 nm could be the result of aggregates formation. A similar phenomenon has been previously noted for tetrapyrroloporphyrazines [17]. Compared to Pcs, tetrapyrroloporphyrazines macrocycles with the same substituents and containing the same central metal cation in the core revealed a higher tendency to form aggregates. In the emission study, macrocycle **2** upon excitation at the Soret as well as the Q band did not emit fluorescence.

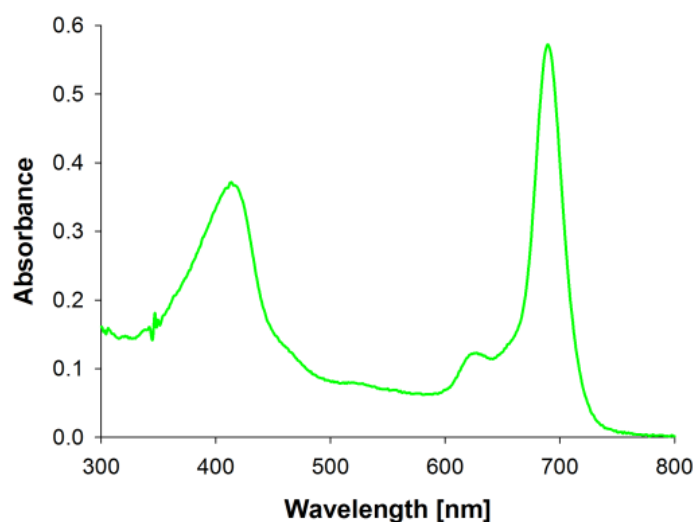


Figure 5. The absorption spectrum of studied compound **2** in DMF.

Tetrapyrazinoporphyrazine derivative **2** revealed low solubility in DMF and DMSO, and it was completely insoluble in the water. Therefore, the quantum yield of singlet oxygen formation was studied only in DMF. An indirect method of singlet oxygen generation was applied using 1,3-diphenylisobenzofuran as a singlet oxygen chemical quencher, whereas an unsubstituted zinc(II) phthalocyanine (ZnPc) was treated as a reference. The mixture of DPBF and tetrapyrazinoporphyrazine derivative **2** was exposed to the monochromatic light at the wavelength adjusted to the maximum of Q band in the absorption spectrum and monitored in time using the UV–Vis spectroscopy. The DPBF decomposition kinetics was calculated and compared with the reference zinc(II) phthalocyanine. The value of the quantum yield of singlet oxygen generation (Φ_{Δ}) approached 0.023. The potential of structurally similar azaphthalocyanine derivative in terms of singlet oxygen generation was previously presented by Mørkved et al. [28]. They reported the quantum yield of singlet oxygen generation of 0.196 for zinc(II) tetrapyrazinoporphyrazine derivative I (Figure 6), which indicates that the thiophenyl functionalization decreased the Φ_{Δ} value as compared to unsubstituted zinc(II) phthalocyanine. Usually, zinc(II) ion-containing phthalocyanine analogs are considered efficient singlet oxygen generators due to the “heavy atom effect” [53]. For example, unsubstituted zinc(II) phthalocyanine used as reference compound reveals significantly higher Φ_{Δ} at the level of 0.56 in DMF and 0.67 in DMSO, whereas unsubstituted magnesium(II) phthalocyanine 0.28 and 0.14, respectively [54]. A similar phenomenon appeared in the case of **2**. An additional issue that could affect a very low singlet oxygen formation by **2** can be combined with terpene moiety. In our latest study, phthalocyanine derivative bearing thymol moieties (II, Figure 6) formed singlet oxygen with the quantum yield of 0.15 in DMF in comparison to unsubstituted zinc(II) phthalocyanine 0.56 [35]. The above-mentioned literature data and the experimental results obtained within current study allow to explain the observed effects. Namely, it seems that the limited singlet oxygen formation ability of **2** can be the result of both magnesium(II) ion presence in the core and bulky methoxy-thiophenyl periphery, which decrease the solubility of studied macrocycle.

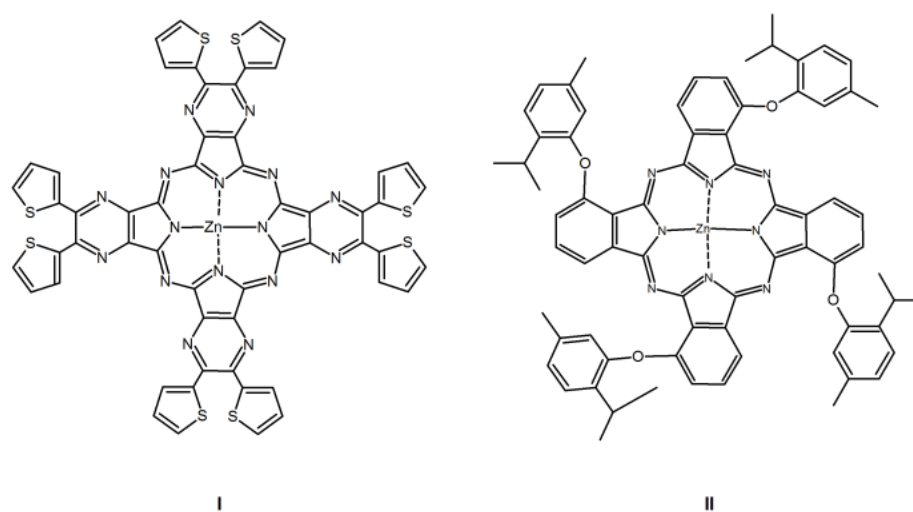


Figure 6. Chemical structures of macrocycles I–II.

In the photostability study, azaphthalocyanine derivative **2** under irradiation with visible light presented very high stability. The calculated quantum yield for photostability (Φ_P) of **2** at 9.59×10^{-6} significantly exceeds the border of 10^{-4} – 10^{-5} , allowing us to classify this macrocycle as a stable porphyrinoid following Dilber and et al. [55]. This time, a high photostability can result from the introduction of menthoxy-thiophenyl moieties in the periphery as a similar phenomenon was observed for phthalocyanine derivative II [35].

4. Conclusions

A novel, symmetrical menthol-thiophenyl substituted tetrapyrrolic macrocycle was synthesized utilizing Lindsey conditions. The optimized synthetic and purification procedures allow us to obtain a new macrocycle with a 36% yield. Tetrapyrrolic macrocycle derivative was subjected to detailed UV-Vis and NMR spectroscopy studies, accompanied by MS spectrometry characteristics. The analysis of the bulky menthol-thiophenyl substituted tetrapyrrolic macrocycle periphery was performed with the use of 1D and 2D NMR techniques and allowed the assigning of the chemical shifts to corresponding hydrogen and carbon atoms.

In the singlet oxygen quantum yield assessment study, tetrapyrrolic macrocycle derivative revealed a low generation of singlet oxygen with a quantum yield of singlet oxygen formation at 2.3% in dimethylformamide. In contrast, in the photostability study, the macrocycle appeared very stable under irradiation with visible light with a quantum yield for photostability of 9.59×10^{-6} in dimethylformamide. Absence of fluorescence emission and very low efficiency of singlet oxygen generation with the value 2.3% allows drawing conclusions on the photophysical and photochemical processes appearing in the Jablonski diagram [56,57]. It especially concerns the elimination of the radiative deactivation pathway of the excited photosensitizer to the ground state by fluorescence. Additionally, it suggests its deactivation by vibrational relaxation which is a non-radiative deactivation process mediated by the interactions between the macrocycle and its surrounding environment. This observation can also be supported by the fact that the deactivation pathway of the excited photosensitizer from its triplet state to the ground state did not occur via singlet oxygen formation pathway.

In summary, our finding is that it is possible to obtain a new [(1R,2S,5R)-2-isopropyl-5-methylcyclohexyloxy]-thiophen-5-yl-substituted tetrapyrrolic macrocycle with magnesium(II) ion, which can be applied in further optical and electrochemical studies.

Supplementary Materials: The following are available online at <https://www.mdpi.com/2076-3417/11/6/2576/s1>.

Author Contributions: Conceptualization, T.G. and L.S.; methodology, S.L., J.T., and B.C.-G.; formal analysis, B.C.-G., T.G., and L.S.; investigation, S.L., J.T., and B.C.-G.; resources, T.G.; data curation, L.S. and S.L.; writing—original draft preparation, S.L., B.C.-G., M.K., and J.M.; writing—review and editing, T.G. and L.S.; supervision, T.G. and L.S.; project administration, S.L. and T.G.; funding acquisition, S.L. All authors have read and agreed to the published version of the manuscript.

Funding: This research was funded by the National Science Centre, Poland through grant No. 2015/19/N/NZ7/01342. The synthesis of 5,6-Bis(2-[(1R,2S,5R)-2-isopropyl-5-methylcyclohexyloxy]-thiophen-5-yl)pyrazine-2,3-dicarbonitrile **1** was supported by the Ministry of Education, Youth and Sports of the Czech Republic (LTAIN19101) for J.T. and M.K.

Institutional Review Board Statement: Not applicable.

Informed Consent Statement: Not applicable.

Conflicts of Interest: The authors declare no conflict of interest.

References

1. Wöhrle, D.; Schnurpfeil, G.; Makarov, S.G.; Kazarin, A.; Suvorova, O.N. Practical Applications of Phthalocyanines—From Dyes and Pigments to Materials for Optical, Electronic and Photo-electronic Devices. *Macroheterocycles* **2012**, *5*, 191–202. [[CrossRef](#)]
2. Huai, M.; Yin, Z.; Wei, F.; Wang, G.; Xiao, L.; Lu, J.; Zhuang, L. Electrochemical CO₂ reduction on heterogeneous cobalt phthalocyanine catalysts with different carbon supports. *Chem. Phys. Lett.* **2020**, *754*, 7655. [[CrossRef](#)]
3. Ma, D.D.; Han, S.G.; Cao, C.; Li, X.; Wu, X.T.; Zhu, Q.L. Remarkable electrocatalytic CO₂ reduction with ultrahigh CO/H₂ ratio over single-molecularly immobilized pyrrolidinonyl nickel phthalocyanine. *Appl. Catal. B Environ.* **2020**, *264*, 8530. [[CrossRef](#)]
4. Mooste, M.; Tkesheliadze, T.; Kozlova, J.; Kikas, A.; Kisand, V.; Treshchalov, A.; Tamm, A.; Aruväli, J.; Zagal, J.H.; Kannan, A.M.; et al. Transition metal phthalocyanine-modified shungite-based cathode catalysts for alkaline membrane fuel cell. *Int. J. Hydrogen Energy* **2021**, *46*, 4365–4377. [[CrossRef](#)]
5. Gounden, D.; Nombona, N.; Van Zyl, W.E. Recent advances in phthalocyanines for chemical sensor, non-linear optics (NLO) and energy storage applications. *Coord. Chem. Rev.* **2020**, *420*, 3359. [[CrossRef](#)]
6. Yano, S.; Hirohara, S.; Obata, M.; Hagiya, Y.; Ogura, S.I.; Ikeda, A.; Kataoka, H.; Tanaka, M.; Joh, T. Current states and future views in photodynamic therapy. *J. Photochem. Photobiol. C Photochem. Rev.* **2011**, *12*, 46–67. [[CrossRef](#)]
7. Sobotta, L.; Mrugalska, S.P.; Mielcarek, J.; Goslinski, T.; Balzarini, J. Photosensitizers Mediated Photodynamic Inactivation against Virus Particles. *Mini-Rev. Med. Chem.* **2015**, *15*, 503–521. [[CrossRef](#)]
8. Sobotta, L.; Mrugalska, S.P.; Piskorz, J.; Mielcarek, J. Porphyrinoid photosensitizers mediated photodynamic inactivation against bacteria. *Eur. J. Med. Chem.* **2019**, *175*, 72–106. [[CrossRef](#)] [[PubMed](#)]
9. Donzello, M.P.; Ercolani, C.; Novakova, V.; Zimcik, P.; Stuzhin, P.A. Tetrapyrrozinoporphyrazines and their metal derivatives. Part I: Synthesis and basic structural information. *Coord. Chem. Rev.* **2016**, *309*, 107–179. [[CrossRef](#)]
10. Novakova, V.; Donzello, M.P.; Ercolani, C.; Zimcik, P.; Stuzhin, P.A. Tetrapyrrozinoporphyrazines and their metal derivatives. Part II: Electronic structure, electrochemical, spectral, photophysical and other application related properties. *Coord. Chem. Rev.* **2018**, *361*, 1–73. [[CrossRef](#)]
11. Donzello, M.P.; Viola, E.; Bergami, C.; Dini, D.; Ercolani, C.; Giustini, M.; Kadish, K.M.; Meneghetti, M.; Monacelli, F.; Rosa, A.; et al. Tetra-2,3-pyrazinoporphyrazines with Externally Appended Pyridine Rings. Chemical and Redox Properties and Highly Effective Photosensitizing Activity for Singlet Oxygen Production of Penta- and Monopalladated Complexes in Dimethylformamide Solution. *Inorg. Chem.* **2008**, *47*, 8757–8766. [[CrossRef](#)]
12. Donzello, M.P.; Viola, E.; Cai, X.; Mannina, L.; Ercolani, C.; Kadish, K.M. Tetra-2,3-pyrazinoporphyrazines with Externally Appended Pyridine Rings. Central (ZnII, CuII, MgII(H₂O), CdII) and Exocyclic (PdII) Metal Ion Binding in Heteropentametallic Complexes from Tetrakis-2,3-[5,6-di(2-pyridyl)pyrazino]porphyrazine. *Inorg. Chem.* **2010**, *49*, 2447–2456. [[CrossRef](#)]
13. Park, J.M.; Song, C.J.; Yao, W.; Jung, C.Y.; Hyun, I.H.; Seong, D.H.; Jaung, J.Y. Synthesis of carbohydrate-conjugated azaphthalocyanine complexes for PDT. *Tetrahedron Lett.* **2015**, *56*, 4967–4970. [[CrossRef](#)]
14. Tomachynskiy, S.; Korobko, S.; Tomachynski, L.; Pavlenko, V. Synthesis and spectral properties of new tetrakis-2,3-[5,7-bis(E)-2-(4-methylphenyl)vinyl]pyrazino]porphyrazine metal complexes. *Opt. Mater.* **2011**, *33*, 1553–1556. [[CrossRef](#)]
15. Lee, B.H.; Jaung, J.Y.; Jang, S.C.; Yi, S.C. Synthesis and optical properties of push–pull type tetrapyrrozinoporphyrazines. *Dye. Pigment.* **2005**, *65*, 159–167. [[CrossRef](#)]
16. Kopecky, K.; Šatinský, D.; Novakova, V.; Miletin, M.; Svoboda, A.; Zimcik, P. Synthesis of mono-, di-, tri- and tetracarboxy azaphthalocyanines as potential dark quenchers. *Dye. Pigment.* **2011**, *91*, 112–119. [[CrossRef](#)]
17. Kostka, M.; Zimcik, P.; Miletin, M.; Klemra, P.; Kopecky, K.; Musil, Z. Comparison of aggregation properties and photodynamic activity of phthalocyanines and azaphthalocyanines. *J. Photochem. Photobiol. A Chem.* **2006**, *178*, 16–25. [[CrossRef](#)]
18. Li, X.; Huang, X.; Gao, R.; Zhang, R.; Zhao, J. Improved performance of Li/SOCl₂ batteries using binuclear metal azaphthalocyanines as electrocatalysts. *Electrochim. Acta* **2016**, *222*, 203–211. [[CrossRef](#)]
19. Alejandro, V.C.; Mónica, F.P.; Xelha, A.P.; Mario, R.; Gabriel, R.O.; Norberto, F.; Eva, R.-G. Brominated BODIPYs as potential photosensitizers for photodynamic therapy using a low irradiance excitation. *Polyhedron* **2020**, *176*, 8. [[CrossRef](#)]

20. Sun, Y.; Yu, X.A.; Yang, J.; Gai, L.; Tian, J.; Sui, X.; Lu, H. NIR halogenated thieno[3, 2-b]thiophene fused BODIPYs with photodynamic therapy properties in HeLa cells. *Spectrochim. Acta Part A Mol. Biomol. Spectrosc.* **2021**, *246*, 9027. [[CrossRef](#)] [[PubMed](#)]
21. Bai, J.; Zhang, L.; Qian, Y. A near-infrared and lysosomal targeting thiophene-BODIPY photosensitizer: Synthesis and its imaging guided photodynamic therapy of cancer cells. *Spectrochim. Acta Part A Mol. Biomol. Spectrosc.* **2021**, *252*, 9512. [[CrossRef](#)]
22. Önal, H.T. Photo Induced Anti-Inflammatory Activities of a Thiophene Substituted Sub-phthalocyanine Derivative. *Photodiagn. Photodyn. Ther.* **2020**, *30*, 1701. [[CrossRef](#)] [[PubMed](#)]
23. Chen, Z.; Zhou, X.; Li, Z.; Niu, L.; Yi, J.; Zhang, F. The third-order optical nonlinearities of thiophene-bearing phthalocyanines studied by Z-scan technique. *J. Photochem. Photobiol. A Chem.* **2011**, *218*, 64–68. [[CrossRef](#)]
24. Sehlotho, N.; Nyokong, T. Electro-catalytic oxidation of thiocyanate, l-cysteine and 2-mercaptoethanol by self-assembled monolayer of cobalt tetraethoxy thiophene phthalocyanine. *Electrochim. Acta* **2006**, *51*, 4463–4470. [[CrossRef](#)]
25. Donzello, M.P.; Ercolani, C.; Stuzhin, P.A. Novel families of phthalocyanine-like macrocycles—Porphyrazines with annulated strongly electron-withdrawing 1,2,5-thia/selenodiazole rings. *Coord. Chem. Rev.* **2006**, *250*, 1530–1561. [[CrossRef](#)]
26. Luo, Q.; Cheng, S.; Tian, H. Synthesis and photochromism of a new binuclear porphyrazinato magnesium(II). *Tetrahedron Lett.* **2004**, *45*, 7737–7740. [[CrossRef](#)]
27. Goslinski, T.; White, A.J. Synthesis, characterization and spectroscopic properties of novel periphery-Functionalized unsymmetrical porphyrazines containing mixed dithienylpyrrolyl and dimethylamino groups. *Polyhedron* **2009**, *28*, 2579–2584. [[CrossRef](#)]
28. Mørkved, E.H.; Andreassen, T.; Novakova, V.; Zimcik, P. Zinc azaphthalocyanines with thiophen-2-yl, 5-methylthiophen-2-yl and pyridin-3-yl peripheral substituents: Additive substituent contributions to singlet oxygen production. *Dye. Pigment.* **2009**, *82*, 276–285. [[CrossRef](#)]
29. Pawełczyk, A.; Kasprzak, S.K.; Olender, D.; Zaprutko, L. Molecular Consortia—Various Structural and Synthetic Concepts for More Effective Therapeutics Synthesis. *Int. J. Mol. Sci.* **2018**, *19*, 1104. [[CrossRef](#)]
30. Boens, N.; Verbelen, B.; Ortiz, M.J.; Jiao, L.; Dehaen, W. Synthesis of BODIPY dyes through postfunctionalization of the boron dipyrromethene core. *Coord. Chem. Rev.* **2019**, *399*, 3024. [[CrossRef](#)]
31. Rizo, F.J.O.; Esnal, I.; Martínez, O.C.A.; Durán, G.C.F.A.; Banuelos, J.; Arbeloa, I.L.; Pannell, K.H.; Magaña, M.A.J.; Cabrera, P.E. 8-Alkoxy- and 8-Aryloxy-BODIPYs: Straightforward Fluorescent Tagging of Alcohols and Phenols. *J. Org. Chem.* **2013**, *78*, 5867–5877. [[CrossRef](#)]
32. Lv, W.; Duan, J.; Ai, S. “Pinwheel-like” phthalocyanines with four non-peripheral chiral menthol units: Synthesis, spectroscopy, and electrochemistry. *Chin. Chem. Lett.* **2019**, *30*, 389–391. [[CrossRef](#)]
33. Romero, M.P.; Gobo, N.R.; De Oliveira, K.T.; Iamamoto, Y.; Serra, O.A.; Louro, S.R. Photophysical properties and photodynamic activity of a novel menthol–zinc phthalocyanine conjugate incorporated in micelles. *J. Photochem. Photobiol. A Chem.* **2013**, *253*, 22–29. [[CrossRef](#)]
34. De Oliveira, K.T.; De Assis, F.F.; Ribeiro, A.O.; Neri, C.R.; Fernandes, A.U.; Baptista, M.S.; Lopes, N.P.; Serra, O.A.; Iamamoto, Y. Synthesis of Phthalocyanines–ALA Conjugates: Water-Soluble Compounds with Low Aggregation. *J. Org. Chem.* **2009**, *74*, 7962–7965. [[CrossRef](#)] [[PubMed](#)]
35. Sobotta, L.; Lijewski, S.; Długaszewska, J.; Nowicka, J.; Mielcarek, J.; Goslinski, T. Photodynamic inactivation of *Enterococcus faecalis* by conjugates of zinc(II) phthalocyanines with thymol and carvacrol loaded into lipid vesicles. *Inorg. Chim. Acta* **2019**, *489*, 180–190. [[CrossRef](#)]
36. Kamatou, G.P.; Vermaak, I.; Viljoen, A.M.; Lawrence, B.M. Menthol: A simple monoterpene with remarkable biological properties. *Phytochemistry* **2013**, *96*, 15–25. [[CrossRef](#)] [[PubMed](#)]
37. Oz, M.; El Nebrisi, E.G.; Yang, K.H.S.; Howarth, F.C.; Al Kury, L.T. Cellular and Molecular Targets of Menthol Actions. *Front. Pharmacol.* **2017**, *8*, 472. [[CrossRef](#)]
38. Pergolizzi, J.V.; Taylor, R.; LeQuang, J.A.; Raffa, R.B.; The NEMA Research Group. The role and mechanism of action of menthol in topical analgesic products. *J. Clin. Pharm. Ther.* **2018**, *43*, 313–319. [[CrossRef](#)]
39. Freires, I.A.; Denny, C.; Benso, B.; De Alencar, S.M.; Rosalen, P.L. Antibacterial Activity of Essential Oils and Their Isolated Constituents against Cariogenic Bacteria: A Systematic Review. *Molecules* **2015**, *20*, 7329–7358. [[CrossRef](#)]
40. Kifer, D.; Mužinić, V.; Klarić, M.Š. Antimicrobial potency of single and combined mupirocin and monoterpenes, thymol, menthol and 1,8-cineole against *Staphylococcus aureus* planktonic and biofilm growth. *J. Antibiot.* **2016**, *69*, 689–696. [[CrossRef](#)]
41. Hloušková, Z.; Tydlitát, J.; Kong, M.; Pytela, O.; Mikysek, T.; Klikar, M.; Almonasy, N.; Dvořák, M.; Jiang, Z.; Růžička, A.; et al. Structure-Catalytic Activity in a Series of Push-Pull Dicyanopyrazine/Dicyanoimidazole Photoredox Catalysts. *Chemics* **2018**, *3*, 4262–4270. [[CrossRef](#)]
42. Sobotta, L.; Fita, P.; Szczolko, W.; Wrotynski, M.; Wierzchowski, M.; Goslinski, T.; Mielcarek, J. Functional singlet oxygen generators based on porphyrazines with peripheral 2,5-dimethylpyrrol-1-yl and dimethylamino groups. *J. Photochem. Photobiol. A Chem.* **2013**, *269*, 9–16. [[CrossRef](#)]
43. Ogunsipe, A.; Durmuş, M.; Atilla, D.; Gürek, A.G.; Ahsen, V.; Nyokong, T. Synthesis, photophysical and photochemical studies on long chain zinc phthalocyanine derivatives. *Synth. Met.* **2008**, *158*, 839–847. [[CrossRef](#)]
44. Seotsanyana-Mokhosi, I.; Kuznetsova, N.A.; Nyokong, T. Photochemical studies of tetra-2,3-pyridinoporphyrazines. *J. Photochem. Photobiol. A Chem.* **2001**, *140*, 215–222. [[CrossRef](#)]

45. Tillo, A.; Stolarska, M.; Kryjewski, M.; Popenda, L.; Sobotta, L.; Jurga, S.; Mielcarek, J.; Goslinski, T. Phthalocyanines with bulky substituents at non-peripheral positions Synthesis and physico-chemical properties. *Dye. Pigment.* **2016**, *127*, 110–115. [[CrossRef](#)]
46. Güzel, E.; Arslan, B.S.; Atmaca, G.Y.; Nebioğlu, M.; Erdoğan, A. High Photosensitized Singlet Oxygen Generating Zinc and Chloroindium Phthalocyanines Bearing (4-isopropylbenzyl)oxy Groups as Potential Agents for Photophysical Applications. *Chemics* **2019**, *4*, 515–520. [[CrossRef](#)]
47. Sobotta, L.; Sniechowska, J.; Ziental, D.; Długaszewska, J.; Potrzebowski, M.J. Chlorins with (trifluoromethyl)phenyl substituents—Synthesis, lipid formulation and photodynamic activity against bacteria. *Dye. Pigment.* **2019**, *160*, 292–300. [[CrossRef](#)]
48. Sobotta, L.; Długaszewska, J.; Kasprzycki, P.; Lijewski, S.; Teubert, A.; Mielcarek, J.; Gdaniec, M.; Goslinski, T.; Fita, P.; Tykarska, E. In vitro photodynamic activity of lipid vesicles with zinc phthalocyanine derivative against *Enterococcus faecalis*. *J. Photochem. Photobiol. B Biol.* **2018**, *183*, 111–118. [[CrossRef](#)]
49. Sobotta, L.; Długaszewska, J.; Gierszewski, M.; Tillo, A.; Sikorski, M.; Tykarska, E.; Mielcarek, J.; Goslinski, T. Photodynamic inactivation of *Enterococcus faecalis* by non-peripherally substituted magnesium phthalocyanines entrapped in lipid vesicles. *J. Photochem. Photobiol. B Biol.* **2018**, *188*, 100–106. [[CrossRef](#)]
50. Härtner, J.; Reinscheid, U.M. Conformational analysis of menthol diastereomers by NMR and DFT computation. *J. Mol. Struct.* **2008**, *872*, 145–149. [[CrossRef](#)]
51. Karplus, M. Vicinal Proton Coupling in Nuclear Magnetic Resonance. *J. Am. Chem. Soc.* **1963**, *85*, 2870–2871. [[CrossRef](#)]
52. Zeng, Q.; Chen, J.; Lin, Y.; Chen, Z. Boosting resolution in NMR spectroscopy by chemical shift upscaling. *Anal. Chim. Acta* **2020**, *1110*, 109–114. [[CrossRef](#)] [[PubMed](#)]
53. Ishii, K. Functional singlet oxygen generators based on phthalocyanines. *Coord. Chem. Rev.* **2012**, *256*, 1556–1568. [[CrossRef](#)]
54. Stolarska, M.; Sobotta, G.A.; Mlynarczyk, D.T.; Długaszewska, J.; Goslinski, T.; Mielcarek, J.; Sobotta, L. Photodynamic Activity of Tribenzoporphyrines with Bulky Periphery against Wound Bacteria. *Int. J. Mol. Sci.* **2020**, *21*, 6145. [[CrossRef](#)]
55. Dilber, G.; Altunparmak, H.; Nas, A.; Kantekin, H.; Durmuş, M. The peripheral and non-peripheral 2H-benzotriazole substituted phthalocyanines: Synthesis, characterization, photophysical and photochemical studies of zinc derivatives. *Spectrochim. Acta Part A Mol. Biomol. Spectrosc.* **2019**, *217*, 128–140. [[CrossRef](#)] [[PubMed](#)]
56. Ng, K.K.; Zheng, G. Molecular Interactions in Organic Nanoparticles for Phototheranostic Applications. *Chem. Rev.* **2015**, *115*, 11012–11042. [[CrossRef](#)] [[PubMed](#)]
57. Oliveira, A.S.; Licsandru, D.; Boscencu, R.; Socoteanu, R.; Nacea, V.; Ferreira, L.F.V. A Singlet Oxygen Photogeneration and Luminescence Study of Unsymmetrically Substituted Mesoporphyrinic Compounds. *Int. J. Photoenergy* **2009**, *2009*, 1–10. [[CrossRef](#)]